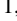






# Data reconstruction of the dynamical connection function in $f(Q)$ cosmology

Yuhang Yang,<sup>1,2,3</sup>  Xin Ren,<sup>1,2,3,4</sup>  Bo wang,<sup>1,2,3</sup>  Yi-Fu Cai<sup>1,2,3</sup>  and Emmanuel N. Saridakis<sup>5,2,6</sup> 

<sup>1</sup>Department of Astronomy, School of Physical Sciences, University of Science and Technology of China, 96 Jinzhai Road, Hefei, Anhui 230026, China

<sup>2</sup>CAS Key Laboratory for Research in Galaxies and Cosmology, School of Astronomy and Space Science,

University of Science and Technology of China, 96 Jinzhai Road, Hefei, Anhui 230026, China

<sup>3</sup>Deep Space Exploration Laboratory, Hefei 230088, China

<sup>4</sup>Department of Physics, Tokyo Institute of Technology, 2-12-1 Ookayama, Meguro-ku, Tokyo 152-8551, Japan

<sup>5</sup>National Observatory of Athens, Lofos Nymfon, 11852 Athens, Greece

<sup>6</sup>Departamento de Matemáticas, Universidad Católica del Norte, Avda. Angamos 0610, Casilla 1280 Antofagasta, Chile

6 September 2024

## ABSTRACT

We employ Hubble data and Gaussian Processes in order to reconstruct the dynamical connection function in  $f(Q)$  cosmology beyond the coincident gauge. In particular, there exist three branches of connections that satisfy the torsionless and curvatureless conditions, parameterized by a new dynamical function  $\gamma$ . We express the redshift dependence of  $\gamma$  in terms of the  $H(z)$  function and the  $f(Q)$  form and parameters, and then we reconstruct it using 55  $H(z)$  observation data. Firstly, we investigate the case where ordinary conservation law holds, and we reconstruct the  $f(Q)$  function, which is very well described by a quadratic correction on top of Symmetric Teleparallel Equivalent of General Relativity. Proceeding to the general case, we consider two of the most studied  $f(Q)$  models of the literature, namely the square-root and the exponential one. In both cases we reconstruct  $\gamma(z)$ , and we show that according to AIC and BIC information criteria its inclusion is favoured compared to both  $\Lambda$ CDM paradigm, as well as to the same  $f(Q)$  models under the coincident gauge. This feature acts as an indication that  $f(Q)$  cosmology should be studied beyond the coincident gauge.

**Key words:** cosmology: observation – cosmology: theory – dark energy

## 1 INTRODUCTION

Since the discovery of the acceleration of the universe expansion in the late 1990's (Riess et al. 1998; Perlmutter et al. 1999), the concept of dark energy (DE) was introduced to explain such an unexpected phenomenon. Although the simplest scenario is just a cosmological constant  $\Lambda$  (Weinberg 1989), resulting to the  $\Lambda$ CDM paradigm, the nature of DE remains puzzling. Hence, the existence of dark sector along with potential observational cosmological tensions (Aghanim et al. 2020a,b; Delubac et al. 2015; Perivolaropoulos & Skara 2022; Abdalla et al. 2022; Di Valentino et al. 2021; Yan et al. 2020; Gangopadhyay et al. 2023), opens the way towards modifications and extensions of the concordance model.

General Relativity (GR) is the standard gravitational theory, and it is based on curvature and the Einstein-Hilbert action (Akrami et al. 2021). Nevertheless, it is known that gravity can be equivalently described through the torsional and non-metricity formulations, namely with Teleparallel Equivalent of General Relativity (TEGR) (Aldrovandi & Pereira 2013) and Symmetric Teleparallel Equivalent of General Relativity (STEGR) (Nester & Yo 1999; Bel-

trán Jiménez et al. 2018b), respectively. Together, these three equivalent formulations constitute the geometric trinity of gravity (Beltrán Jiménez et al. 2019; Capozziello et al. 2022). Modifications of curvature-based General Relativity directly lead to the well-known  $f(R)$  gravity (Starobinsky 1980; Capozziello 2002), to  $f(G)$  gravity (Nojiri & Odintsov 2005), to Lovelock gravity (Lovelock 1971), etc. Furthermore, the extension of TEGR, known as  $f(T)$  gravity, has been well discussed and studied in cosmology (Cai et al. 2016, 2018; Krssak et al. 2019; Yan et al. 2020; Huang et al. 2022; Wang et al. 2024; Hu et al. 2023). Finally, modifications based on the non-metricity scalar  $Q$ , i.e. extensions of the STEGR, lead to  $f(Q)$  gravity (Beltrán Jiménez et al. 2018b; Heisenberg 2024). The cosmological applications of  $f(Q)$  gravity prove to be very interesting, and thus they have recently attracted a large amount of research (Khyllip et al. 2021; Mandal et al. 2020; Barros et al. 2020; Järv et al. 2018; Lu et al. 2019; De & How 2022; Solanki et al. 2022; Lympers 2022; D'Ambrosio et al. 2022b; Li & Zhao 2022; Dimakis et al. 2021; Hohmann 2021; Kar et al. 2022; Wang et al. 2022; Quiros 2022; Mandal & Sahoo 2021; Albuquerque & Frusciante 2022; Capozziello & D'Agostino 2022; Capozziello & Shokri 2022; Dimakis et al. 2022b; D'Agostino & Nunes 2022; Narawade & Mishra 2023; Emtsova et al. 2023; Bahamonde et al. 2023; Bahamonde & Järv 2022; Sokoliuk et al. 2023; De et al. 2024; Dimakis et al. 2023; Maurya et al. 2023; Ferreira et al. 2023; Capozziello et al. 2023; Koussour & De 2023; Nájera et al. 2023; Atayde & Frusciante 2023; Paliathanasis et al.

\* E-mail: yyh1024@mail.ustc.edu.cn

† E-mail: rx76@ustc.edu.cn

‡ E-mail: ymwangbo@ustc.edu.cn

§ E-mail: yifucai@ustc.edu.cn

¶ E-mail: msaridak@noa.gr

2024; Bhar 2023; Mussatayeva et al. 2023; Paliathanasis 2024; Mandal et al. 2023; Pradhan et al. 2024; Capozziello et al. 2024; Bhar et al. 2024; Mhamdi et al. 2024; Gonçalves et al. 2024). We mention that recently there is a discussion whether  $f(Q)$  gravity exhibits the strong coupling or ghost presence (Gomes et al. 2024), nevertheless one can construct versions of the theory that are free from these issues, incorporating non-minimal couplings or direct couplings of the matter field to the connection (Heisenberg 2024; Heisenberg et al. 2024; D'Ambrosio et al. 2023).

While the coincident gauge is commonly used in  $f(Q)$  cosmology, exploring the general covariant formulation provides additional forms of affine connections (Zhao 2022; Hohmann 2021). Generally, there are three possible branches of connections satisfying the torsionless and curvatureless conditions, introducing a free dynamical function  $\gamma(t)$ , which affects the solutions of the theory (D'Ambrosio et al. 2022a; Heisenberg et al. 2023; Dimakis et al. 2022a; Shabani et al. 2024; Paliathanasis et al. 2024; Dimakis et al. 2022b). One of the three branches is equivalent to the coincident gauge in cartesian Friedmann-Robertson-Walker metric (Hohmann 2021), while the other two exhibit distinct dynamical behavior when  $\gamma(t)$  is non-vanishing. Therefore, it is of great significance to study the physical properties and evolutionary characteristics of parameter  $\gamma(t)$  in  $f(Q)$  gravity.

In this work, we are interesting in investigating the dynamical connection function  $\gamma(t)$  of the covariant  $f(Q)$  cosmology, from the data perspective. There is no physical motivation to determine the functional form of  $\gamma(t)$ . In particular, we desire to reconstruct it from the data without any assumption of its functional form, in contrast to previous studies (Shi 2023; Subramaniam et al. 2023). For this sake, we employ Gaussian Processes (GP) for data reconstruction, a technique widely used in cosmology, allowing us to directly obtain reconstruction functions from observational Hubble parameter data (Cai et al. 2020; Seikel et al. 2012; Ren et al. 2021, 2022; Levi Said et al. 2021; Bonilla et al. 2022; Bernardo & Levi Said 2021; Elizalde et al. 2024; Yu et al. 2018). Subsequently, we analyze the evolution characteristics of the connection function and its influence on the dynamics of the universe in different branches.

This article is structured as follows. In Section 2 we present a concise introduction to covariant  $f(Q)$  gravity and cosmology. Then, in Section 3 we reconstruct the connection function  $\gamma(t)$  from the data. In particular, in subsection 3.1 we display the data list that we use, and we describe the Gaussian Process that we apply. Then, in subsection 3.2 we perform the reconstruction procedure assuming the ordinary conservation law for the matter sector, while in subsection 3.3 we present the reconstruction results in the general case, considering two specific  $f(Q)$  models that are the most well studied in the literature. Finally we draw the conclusions and provide some discussion in Section 4.

## 2 $F(Q)$ GRAVITY AND COSMOLOGY

In this section we briefly review  $f(Q)$  gravity and its application in cosmology. In  $f(Q)$  gravity, metric and connection are treated on equal footing, necessitating the use of the Palatini formalism to describe gravitational interaction (Beltrán Jiménez et al. 2018a). In this formalism, a general affine connection  $\Gamma^\alpha_{\mu\nu}$  is introduced and defined as

$$\Gamma^\alpha_{\mu\nu} = \overset{\circ}{\Gamma}^\alpha_{\mu\nu} + L^\alpha_{\mu\nu}, \quad (1)$$

where  $\overset{\circ}{\Gamma}^\alpha_{\mu\nu}$  is the Levi-Civita connection, and the  $L^\alpha_{\mu\nu}$  characterizes the deviation of the full affine connection from the Levi-Civita one.

In the following, we use the upper ring to represent that the geometric quantity is calculated under the Levi-Civita connection. Note that we do not consider the anti-symmetry part of the connection, since the theory encompasses a torsion-free geometry. The affine connection  $\Gamma^\alpha_{\mu\nu}$  establishes the affine structure, governing how tensors should be transformed, and defining the covariant derivative  $\nabla_\alpha$ .

Utilizing this general affine connection, we define the basic object in this theory, the non-metricity tensor, as  $Q_{\alpha\mu\nu} = \nabla_\alpha g_{\mu\nu}$ , which characterizes the geometry of spacetime. Moreover, the disformation tensor  $L^\alpha_{\mu\nu}$  can be expressed as:

$$L^\alpha_{\mu\nu} = \frac{1}{2}(Q^\alpha_{\mu\nu} - Q^\alpha_{\nu\mu} - Q^\alpha_{\nu\mu}). \quad (2)$$

By imposing the condition of vanishing curvature, the non-metricity scalar can be extracted as

$$Q = \frac{1}{4}Q^\alpha Q_\alpha - \frac{1}{2}\tilde{Q}^\alpha Q_\alpha - \frac{1}{4}Q_{\alpha\mu\nu}Q^{\alpha\mu\nu} + \frac{1}{2}Q_{\alpha\mu\nu}Q^{\nu\mu\alpha}, \quad (3)$$

where  $Q_\alpha = g^{\mu\nu}Q_{\alpha\mu\nu}$  and  $\tilde{Q}_\alpha = g^{\mu\nu}Q_{\mu\alpha\nu}$  represent the two independent traces of the non-metricity tensor. It is convenient to introduce the non-metricity conjugate tensor  $P^\alpha_{\mu\nu}$  as

$$P^\alpha_{\mu\nu} = \frac{1}{4} \left( -2L^\alpha_{\mu\nu} + Q^\alpha g_{\mu\nu} - \tilde{Q}^\alpha g_{\mu\nu} - \frac{1}{2}\delta^\alpha_\mu Q_\nu - \frac{1}{2}\delta^\alpha_\nu Q_\mu \right), \quad (4)$$

which allows the non-metricity scalar to be simplified as  $Q = Q_{\alpha\mu\nu}P^{\alpha\mu\nu}$ .

We can now use the non-metricity scalar  $Q$  to construct  $f(Q)$  gravity, introducing the action

$$S = \int d^4x \sqrt{-g} \left[ \frac{1}{2}f(Q) + \mathcal{L}_m \right], \quad (5)$$

where  $g$  is the determinant of the metric,  $f(Q)$  is an arbitrary function of  $Q$ ,  $\mathcal{L}_m$  is the matter Lagrangian density, and here we have set the gravitational constant  $8\pi G = 1$ . It is worth noting that STEGR, and therefore GR, is recovered for  $f(Q) = Q$ . Finally, as usual, we define the energy-momentum tensor of matter as

$$T_{\mu\nu} = -\frac{2}{\sqrt{-g}} \frac{\delta(\sqrt{-g}\mathcal{L}_m)}{\delta g^{\mu\nu}}. \quad (6)$$

Variation of the above action with respect to the metric leads to the metric field equation:

$$T_{\mu\nu} = \frac{2}{\sqrt{-g}} \nabla_\lambda \left( \sqrt{-g} f_Q P^\lambda_{\mu\nu} \right) - \frac{1}{2} f g_{\mu\nu} + f_Q (P_{\nu\rho\sigma} Q^\rho_{\mu\sigma} - 2P_{\rho\sigma\mu} Q^\rho_{\nu\sigma}), \quad (7)$$

where  $f_Q = df/dQ$ ,  $f_{QQ} = d^2f/dQ^2$ . Alternatively, it can be expressed in a covariant formulation to highlight the distinction from GR more clearly, namely (Subramaniam et al. 2023; Beh et al. 2022; Zhao 2022):

$$f_Q \overset{\circ}{G}_{\mu\nu} + \frac{1}{2} g_{\mu\nu} (f_Q Q - f) + 2f_{QQ} P^\lambda_{\mu\nu} \overset{\circ}{\nabla}_\lambda Q = T_{\mu\nu}, \quad (8)$$

where  $\overset{\circ}{G}_{\mu\nu} = \overset{\circ}{R}_{\mu\nu} - \frac{1}{2} g_{\mu\nu} \overset{\circ}{R}$  is the standard the Einstein tensor and  $\overset{\circ}{\nabla}_\lambda$  is the covariant derivative corresponding to Levi-Civita connection. From this formula we can easily see that in more general cases where  $f(Q)$  is not a linear function of  $Q$ , the affine connection will enter the dynamics of the metric, ultimately affecting the solutions.

Variation of action (5) with respect to the connection gives

$$4\nabla_\mu \nabla_\nu (\sqrt{-g} f_Q P^{\mu\nu}_\alpha) = -\nabla_\mu \nabla_\nu (\sqrt{-g} H^\mu_\alpha), \quad (9)$$

**Table 1.** Three different branches of time-dependent functions  $C_1$ ,  $C_2$  and  $C_3$  with vanishing curvature and torsion, where  $\gamma(t)$  is a non-vanishing dynamical function, and with dots denoting time derivatives.

Case	$C_1$	$C_2$	$C_3$
Connection I	$\gamma$	0	0
Connection II	$\gamma + \frac{\dot{\gamma}}{\gamma}$	0	$\gamma$
Connection III	$-\frac{\dot{\gamma}}{\gamma}$	$\gamma$	0

where we have introduced the hypermomentum tensor density

$$H_{\alpha}^{\mu\nu} = -\frac{2}{\sqrt{-g}} \frac{\delta(\sqrt{-g}\mathcal{L}_m)}{\delta\Gamma^{\alpha}_{\mu\nu}}. \quad (10)$$

Finally, using the Bianchi identities, the above connection field equation leads to the energy-momentum-hypermomentum conservation law, namely (Harko et al. 2018; Hohmann 2021; Iosifidis 2021, 2020)

$$\sqrt{-g}\overset{\circ}{\nabla}_{\nu}T_{\mu}^{\nu} = -\frac{1}{2}\overset{\circ}{\nabla}_{\nu}\overset{\circ}{\nabla}_{\rho}(\sqrt{-g}H_{\mu}^{\nu\rho}). \quad (11)$$

We proceed to the application of  $f(Q)$  gravity at a cosmological framework. Thus, we consider the isotropic and homogeneous flat Friedmann-Robertson-Walker (FRW) metric

$$ds^2 = -dt^2 + a(t)^2(dr^2 + r^2d\theta^2 + r^2\sin^2\theta d\phi^2), \quad (12)$$

with  $a(t)$  the scale factor. As we mentioned in the Introduction, most studies in  $f(Q)$  cosmology were conducted within the coincident gauge choice, where all connection coefficients vanish, namely  $\Gamma^{\alpha}_{\mu\nu} = 0$ . Nevertheless, this is not the only choice (Hohmann 2021), and therefore there are some recent studies which use different connections in  $f(Q)$  cosmology (Subramaniam et al. 2023; Hohmann 2021; D'Ambrosio et al. 2022a; Heisenberg et al. 2023; Dimakis et al. 2022a; Shi 2023; Paliathanasis et al. 2024; Jarv & Pati 2024; Dimakis et al. 2022b).

In general, the nonzero components of a torsionless connection in flat FRW universe are (Hohmann 2020):

$$\begin{aligned} \Gamma^t_{tt} &= C_1, & \Gamma^r_{rr} &= C_2, & \Gamma^t_{\theta\theta} &= C_2r^2 & \Gamma^t_{\phi\phi} &= C_2r^2\sin^2\theta, \\ \Gamma^r_{tr} &= C_3, & \Gamma^r_{rr} &= 0, & \Gamma^r_{\theta\theta} &= -r, & \Gamma^r_{\phi\phi} &= -r\sin^2\theta, \\ \Gamma^{\theta}_{t\theta} &= C_3, & \Gamma^{\theta}_{r\theta} &= \frac{1}{r}, & \Gamma^{\theta}_{\phi\phi} &= -\cos\theta\sin\theta, \\ \Gamma^{\phi}_{t\phi} &= C_3, & \Gamma^{\phi}_{r\phi} &= \frac{1}{r}, & \Gamma^{\phi}_{\theta\phi} &= \cot\theta, \end{aligned} \quad (13)$$

where  $C_1, C_2, C_3$  are purely temporal functions. As one can show, in total there are three possible branches of such connections that satisfy additionally the curvatureless requirement, which are presented in Table 1, where  $\gamma$  is a non-vanishing function on  $t$ .

In the case of FRW metric, with the above general connection parameterization, one can calculate the non-metricity scalar from (3) as

$$Q(t) = 3 \left[ -2H^2 + 3C_3H + \frac{C_2}{a^2}H - (C_1 + C_3)\frac{C_2}{a^2} + (C_1 - C_3)C_3 \right], \quad (14)$$

where  $H = \frac{\dot{a}}{a}$  is the Hubble function. Note that when one goes back to the case of zero connection, the above expression yields the standard result  $Q(t) = -6H^2$ , while for our three connections of Table 1 we

obtain

$$Q(t) = -6H^2 \quad \text{for Connection I,} \quad (15)$$

$$Q(t) = 3 \left( -2H^2 + 3\gamma H + \dot{\gamma} \right) \quad \text{for Connection II,} \quad (16)$$

$$Q(t) = 3 \left( -2H^2 + \frac{\gamma}{a^2}H + \frac{\dot{\gamma}}{a^2} \right) \quad \text{for Connection III.} \quad (17)$$

Substituting the above general connection into the field equations (7), and introducing for convenience the ansatz  $f(Q) = Q + F(Q)$ , we obtain the modified Friedmann equations as

$$\rho_m - \frac{1}{2}F + \left(\frac{1}{2}Q - 3H^2\right)F_Q - \frac{3}{2}\dot{Q}(C_3 - \frac{C_2}{a^2})F_{QQ} = 3H^2, \quad (18)$$

$$\begin{aligned} p_m + \frac{1}{2}F + (2\dot{H} + 3H^2 - \frac{1}{2}Q)F_Q - \frac{1}{2}\dot{Q}(-4H + 3C_3 + \frac{C_2}{a^2})F_{QQ} \\ = -2\dot{H} - 3H^2, \end{aligned} \quad (19)$$

where a subscript  $Q$  denotes differentiation with respect to  $Q$ . In the above equations,  $\rho_m$  and  $p_m$  are the energy density and pressure of the (baryonic plus cold dark matter) matter sector, assuming it to correspond to a perfect fluid. Note that we do not consider the radiation sector since we focus on late-time universe. Comparing the above Friedmann equations with the standard ones, we can see that in the scenario at hand we obtain an effective dark energy sector with energy density and pressure respectively given by

$$\rho_{de} = -\frac{1}{2}F + \left(\frac{1}{2}Q - 3H^2\right)F_Q - \frac{3}{2}\dot{Q}(C_3 - \frac{C_2}{a^2})F_{QQ}, \quad (20)$$

$$p_{de} = \frac{1}{2}F + (2\dot{H} + 3H^2 - \frac{1}{2}Q)F_Q - \frac{1}{2}\dot{Q}(-4H + 3C_3 + \frac{C_2}{a^2})F_{QQ}, \quad (21)$$

and thus with an effective equation-of-state parameter written as

$$\begin{aligned} w_{de} &= \frac{p_{de}}{\rho_{de}} \\ &= \frac{\frac{1}{2}F + (2\dot{H} + 3H^2 - \frac{1}{2}Q)F_Q - \frac{1}{2}\dot{Q}(-4H + 3C_3 + \frac{C_2}{a^2})F_{QQ}}{-\frac{1}{2}F + (\frac{1}{2}Q - 3H^2)F_Q - \frac{3}{2}\dot{Q}(C_3 - \frac{C_2}{a^2})F_{QQ}}. \end{aligned} \quad (22)$$

Lastly, let us make some comments on the the conservation law in  $f(Q)$  gravity. As one can see from equation (11), this relation remains independent of the gravitational part, depending only on the matter terms. The left hand side in the case of FRW metric gives as usual  $\overset{\circ}{\nabla}_{\nu}T_{\mu}^{\nu} = [\dot{\rho}_m + 3H(\rho_m + p_m)]u_{\mu}$ . In the case of zero connection, where the hypermomentum is absent, the right hand side disappears, and thus equation (11) gives  $\dot{\rho}_m + 3H(\rho_m + p_m) = 0$  as expected. However, for the general connection choices given in Table 1 the hypermomentum is not always vanish, and thus the dynamical function  $\gamma(t)$  will enter the right hand side leading to a non-conservation of the matter sector. In other words we obtain an effective interaction between the connection structure of the geometry and the matter sector, which is typical in more complicated geometries (Ikeda et al. 2019; Papagiannopoulos et al. 2017; Konitopoulos et al. 2021; Savvopoulos & Stavrinos 2023).

Under Connection I of Table 1, the scenario is consistent with the standard approach in  $f(Q)$  cosmology, where the coincident gauge with vanishing affine connections is used. As a result, the unknown dynamical function  $\gamma$  does not play any role in the evolution of the universe at the background level, and this is the aspect which previous studies have focused on. However, the situation changes when one considers the remaining two types of connections. From the modified Friedmann equations (18),(19), it is evident that  $\gamma$  enters as

a new dynamical field, and thus its evolution will affect the universe dynamics at the background level. Furthermore, as we mentioned above, from equation (11) we deduce that  $\gamma$  will play a role in the matter equation, too. We mention here that for different models the evolution feature of  $\gamma$  will be different. In the next section we will investigate these particular effects in detail for some specific models, and we will perform a confrontation with observational data.

### 3 RECONSTRUCTING THE DYNAMICAL CONNECTION FUNCTION $\gamma(T)$ FROM THE DATA

In this section we desire to explore the effect of Connection II and Connection III on the background evolution, and in particular to use observational data in order to reconstruct  $\gamma(t)$ . In order to achieve that we will apply Gaussian Processes, since this procedure ensures model-independence and thus it will provide insights into the characteristics of  $\gamma$  and its impact on the cosmological evolution within the framework of general covariant symmetric teleparallel theory.

#### 3.1 Hubble data set

Since in the following we will apply a reconstruction procedure based on  $H(z)$ , in this work we will use  $H(z)$  data from the observational Hubble data (OHD) list, gathered from several studies (Farooq et al. 2017; Zhang & Xia 2016; Yu et al. 2018; Magana et al. 2018). The  $H(z)$  data in this list are primarily derived from cosmic chronometer (CC) and radial baryon acoustic oscillations (BAO) observations. Cosmic chronometer yields  $H(z)$  information by measuring age differences between two galaxies at distinct redshifts, evolving independently of any specific model (Jimenez & Loeb 2002). On the other hand, radial BAO observations involve pinpointing the BAO peak position in galaxy clustering, relying on the sound horizon in the early universe (Alam et al. 2017; Zhao et al. 2017). In summary, the data list is composed of 31 CC data points and 23 radial BAO data points, as documented in (Li et al. 2021). Finally, for the current value of the Hubble function  $H_0$  we adopt the most recent SH0ES observation of  $73.04 \pm 1.04 \text{ km s}^{-1} \text{ Mpc}^{-1}$  (Riess et al. 2022).

However, the discontinuity in data points with error bars, in general affects the smoothness of the reconstructed functions. To address this issue we employ Gaussian Processes in Python (GAPP), and thus we result to a continuous  $H(z)$  function that best fits our discrete data. GP have been widely used for the parameter or function reconstruction in various studies (Cai et al. 2020; Seikel et al. 2012; Ren et al. 2021, 2022; Levi Said et al. 2021; Bonilla et al. 2022; Bernardo & Levi Said 2021; Elizalde et al. 2024; Yu et al. 2018). Concerning the covariance function in GAPP, for the kernel choice in our analysis we select the exponential form, namely:

$$k(x, x') = \sigma_f^2 e^{-\frac{(x-x')^2}{2l^2}}, \quad (23)$$

where  $\sigma_f$  and  $l$  are the hyperparameters.

We apply the GAPP steps, and we obtain a reconstructed  $H(z)$  function, which is depicted in Figure 1. The orange curve represents the mean value, while the light yellow shaded zones indicate the allowed regions at  $1\sigma$  confidence level.

#### 3.2 Reconstruction for the matter conservation case

We will start our analysis for the case where there is no interaction between the geometry and matter, and thus matter is conserved,

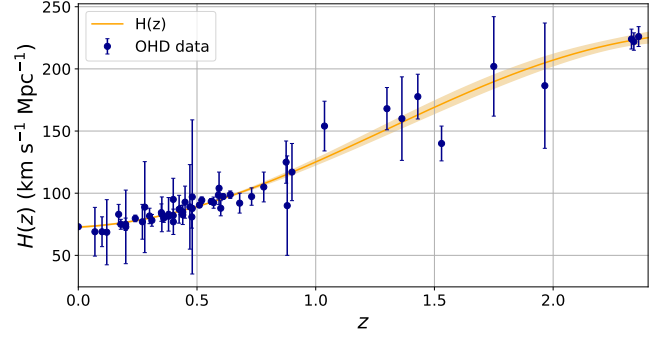


**Figure 1.** The reconstructed  $H(z)$  function arising from the 55 data points through Gaussian Processes, imposing  $H_0 = 73.04 \pm 1.04 \text{ km s}^{-1} \text{ Mpc}^{-1}$ . The orange curve denotes the mean value, while the light yellow shaded zones indicate the allowed regions at  $1\sigma$  confidence level.

namely we will focus on the case where the general conservation equation (11) gives the ordinary conservation law (OCL)

$$\dot{\rho}_m + 3H(\rho_m + p_m) = 0. \quad (24)$$

Manipulating the Friedmann equations (18),(19) we find

$$\begin{aligned} & \dot{\rho}_m + 3H(\rho_m + p_m) \\ &= \dot{Q} \left[ -3H^2 - \frac{1}{2}Q + \frac{3}{2} \left( C_3 - \frac{C_2}{a^2} \right) + 9C_3H - \frac{3C_2}{a^2}H \right] \\ & \quad + \frac{3}{2}Q\ddot{Q} \left( C_3 - \frac{C_2}{a^2} \right) F_{QQ} + \frac{3}{2}\dot{Q}^2 \left( C_3 - \frac{C_2}{a^2} \right) F_{QQQ}. \end{aligned} \quad (25)$$

Connection I will lead to trivial results, since  $\gamma$  disappears from the equations. Let us consider connection II of Table 1. In this case, enforcing the OCL condition, i.e. enforcing the right-hand-side of the above equation to be zero, and using (16), we obtain  $(\frac{9}{2}\gamma H\dot{Q} + \frac{3}{2}\dot{Q}\ddot{Q})F_{QQ} + \frac{3}{2}\dot{Q}^2\gamma F_{QQQ} = 0$ . Thus, applying the chain rules  $F'_Q = F_{QQ}\dot{Q}$  and  $F''_Q = F_{QQQ}\dot{Q}^2 + F_{QQ}\ddot{Q}$ , we finally acquire (Shabani et al. 2023)

$$F''_Q + 3HF'_Q = 0. \quad (26)$$

In the following it is more convenient to use the redshift  $z$  as the independent variable, through  $dz/dt = -(1+z)H(z)$ . Hence, one can easily obtain the general solution for equation (26) as

$$F_Q = A \int a^{-3} dt + B = -A \int \frac{(1+z)^2}{H(z)} dz + B, \quad (27)$$

where  $A$  and  $B$  are constants. Lastly, note that in the case of Connection III the equations are too complicated to accept analytical solutions, and hence we will not consider it further.

Equation (27) is our first dynamical equation. The second one will arise from the Friedmann equations (18),(19), which yield

$$-2H' \frac{dz}{dt} - \rho_m - p_m = 2H' F_Q \frac{dz}{dt} - (3\gamma - 2H) F'_Q \frac{dz}{dt}, \quad (28)$$

where primes denote derivatives with respect to  $z$ . Finally, the third dynamical equation is the OCL (24). These three dynamical equations for the three unknown functions, namely  $H(z)$ ,  $\rho_m(z)$  and  $\gamma(z)$  can be easily solved in the case of dust matter, namely imposing  $p_m = 0$ . In this case we obtain

$$\gamma(z) = \frac{2HH'}{3A(1+z)^2} \left[ A \int_0^z \frac{(1+z')^2}{H(z')} dz' - B - 1 \right] + \frac{2}{3}H(z) + \frac{\Omega_{m0}H_0^2}{A}, \quad (29)$$



where  $\Omega_{m0}$  is the present value of the matter density parameter  $\Omega_m \equiv \rho_m/(3H^2)$ . Note that in the case  $A = 0$  the presence of  $\gamma$  has no impact on the background evolution, and moreover in such a case (27) leads to a linear  $f(Q)$  form, which is consistent with our previous discussion that in the standard STEGR case (where  $f(Q)$  is simply linear in  $Q$ ) OCL condition holds naturally. In the following we focus on the general case where  $A \neq 0$ .

Since  $F_Q$  is dimensionless, it proves convenient to parameterize  $A$  as  $A = \epsilon H_0$ , with  $\epsilon$  a dimensionless parameter and  $H_0$  the current value of the Hubble function. Additionally, the integration constant  $B$  in (27) yields a linear term in  $f(Q)$ , which can always be absorbed in a redefinition of the gravitational constant, and hence it can be set arbitrarily. Without loss of generality, for calculation convenience, in the following we set it to  $B = -5$ .

Let us now proceed to the reconstruction procedure. In (29) we extracted  $\gamma(z)$  in terms of  $H(z)$ , while in the previous subsection, and in particular in Figure 1, we reconstructed  $H(z)$  from the data. Thus, we can easily reconstruct  $\gamma(z)$  itself. In Figure 2(a), 2(b) we present the reconstruction results of  $\gamma(z)$  and  $Q(z)$  for different values of  $\epsilon$ . As we observe, with the increase of  $\epsilon$  values, the reconstruction results converge to a certain curve, while the value of  $\gamma$  at current time is  $8H'_0/3\epsilon + 2H_0/3 + \Omega_{m0}H_0/\epsilon$ . Additionally, as the value of  $\epsilon$  increases, the value of  $Q$  no longer decreases monotonically with the expansion of the universe, but instead a minimum value appears in the course of evolution. In the late-time universe,  $Q$  appears to evolve independently of the choice of  $\epsilon$ , which implies that the influence of the existence of  $\gamma$  on the universe evolution will diminish progressively.

In the same lines, using (27) we can reconstruct  $F_Q(z)$ , while from (16) we can reconstruct  $Q(z)$ , thus obtaining in the end the reconstruction of  $F(Q)$ , which is depicted in Figure 2(c). Interestingly enough, this function deviates from the linear form, hence we deduce that the data favour a deviation from standard STEGR, i.e. from standard General Relativity. In particular, taking  $\epsilon = 2$  as an example, we find that the best fit function is the one with a quadratic correction, namely

$$F(Q) = a_1 + a_2 \frac{Q}{Q_0} + a_3 \frac{Q^2}{Q_0^2}, \quad (30)$$

with  $a_1 = -34614$ ,  $a_2 = 65317$ , and  $a_3 = 724$ , and where the current value of  $Q$  is  $Q_0 = -8009$ , in  $H_0^2$  units. The fact that the quadratic correction fits the data very efficiently, and is favoured comparing to standard General Relativity, is one of the main results of the present work.

### 3.3 Reconstruction in the general case

Let us now proceed to the general case, in which the general conservation law (11) implies an interaction between matter and geometry. In this case it is necessary to impose an ansatz for the  $f(Q)$  function, and thus in the following we will focus on the two most studied models of the literature.

The first model is abbreviated as Sqrt- $f(Q)$  model, and has the form (Frusciante 2021)

$$F(Q) = M\sqrt{-Q} - 2\Lambda, \quad (31)$$

where  $M, \Lambda$  are free parameters. To render this expression dimensionless, we introduce a parameter  $\alpha = M/H_0$ , yielding the form  $F(Q) = (\alpha H_0)\sqrt{-Q} - 2\Lambda$ . In the coincident gauge, this model reproduces the same background evolution with  $\Lambda$ CDM scenario. However, the distinctive effects of varying  $\alpha$  become discernible by

analyzing the evolution of perturbations in the coincident gauge (Barros et al. 2020; Frusciante 2021; Atayde & Frusciante 2021; Ferreira et al. 2022). It remains an open question whether these conclusions hold in more general connections, as explored in (Subramaniam et al. 2023), where the authors investigate the energy conditions under different assumptions on the form of  $\gamma$ .

The second model is abbreviated Exp- $f(Q)$  model, and has the form (Anagnostopoulos et al. 2021)

$$F(Q) = Qe^{\beta \frac{Q_0}{Q}} - Q, \quad (32)$$

where  $\beta$  is a dimensionless free parameter, and  $Q_0$  the value of  $Q$  at current time. This model exhibits a remarkable capability to effectively align with observations, and in some cases it is favoured comparing to  $\Lambda$ CDM scenario, although it does not contain an explicit cosmological constant (Anagnostopoulos et al. 2021; Khyllip et al. 2023; Lympetis 2022; Ferreira et al. 2023). Moreover, it effortlessly satisfies Big Bang Nucleosynthesis (BBN) constraints (Anagnostopoulos et al. 2023), since at early times, where  $Q \gg Q_0$ , it coincides with General Relativity. Once again we mention that these results stem from analyses conducted in the coincident gauge, prompting further investigation into their applicability in more general connections.

Let us proceed to the reconstruction of the connection function  $\gamma(z)$ . From the Friedmann equations (18),(19) we find that

$$\dot{Q} = \frac{F + 2(2\dot{H} + 3H^2)(F_Q + 1) - QF_Q}{(-4H + 3C_3 + \frac{C_2}{a^2})F_{QQ}}. \quad (33)$$

Similarly to the previous subsection, we will not consider Connection I, since in this case  $\gamma$  does not affect the equations. For the other two connections, taking the time derivative of (16),(17) yields:

$$\dot{Q} = -12H\dot{H} + 9\dot{\gamma}H + 9\gamma\dot{H} + 3\ddot{\gamma} \quad \text{for Connection II,} \quad (34)$$

$$\dot{Q} = -12H\dot{H} + \frac{3\ddot{\gamma} + 3\gamma\dot{H} - 3\dot{\gamma}H - 6\gamma H^2}{a^2} \quad \text{for Connection III.} \quad (35)$$

Comparing eq. (33) with (34) and (35), leads to

$$\ddot{\gamma} = \frac{F + 2(2\dot{H} + 3H^2)(F_Q + 1) - QF_Q}{3(-4H + 3\gamma)F_{QQ}} + 4H\dot{H} - 3\dot{\gamma}H - 3\gamma\dot{H}, \quad (36)$$

for Connection II and

$$\ddot{\gamma} = a^2 \left[ \frac{F + 2(2\dot{H} + 3H^2)(F_Q + 1) - QF_Q}{3\left(\frac{\gamma}{a^2} - 4H\right)F_{QQ}} + 4H\dot{H} \right] + 2\gamma H^2 + \dot{\gamma}H - \gamma\dot{H}, \quad (37)$$

for Connection III. Hence, changing the cosmic time  $t$  to redshift  $z$  through  $dz/dt = -(1+z)H(z)$ , we are now able to reconstruct the evolution  $\gamma(z)$  using the observationally reconstructed  $H(z)$  of Figure 1. It can be seen from eq. (36) and eq. (37) that the reconstruction of parameter  $\gamma(z)$  depends on the specific function form of  $f(Q)$ . We mention here that in the literature one can find the observational constraints for Sqrt- $f(Q)$  model and Exp- $f(Q)$  model, however only for the case of zero connection (coincident gauge). Therefore, since in the present work we focus on non-zero  $\gamma$ , the model parameters (namely  $\alpha, \Lambda$  for the first model and  $\beta$  for the second model respectively) should be considered as free parameters from scratch.

We start from the case of Connection II. In the upper panels of Figure 3 we present the reconstruction results of  $\gamma(z)$ , for Sqrt- $f(Q)$

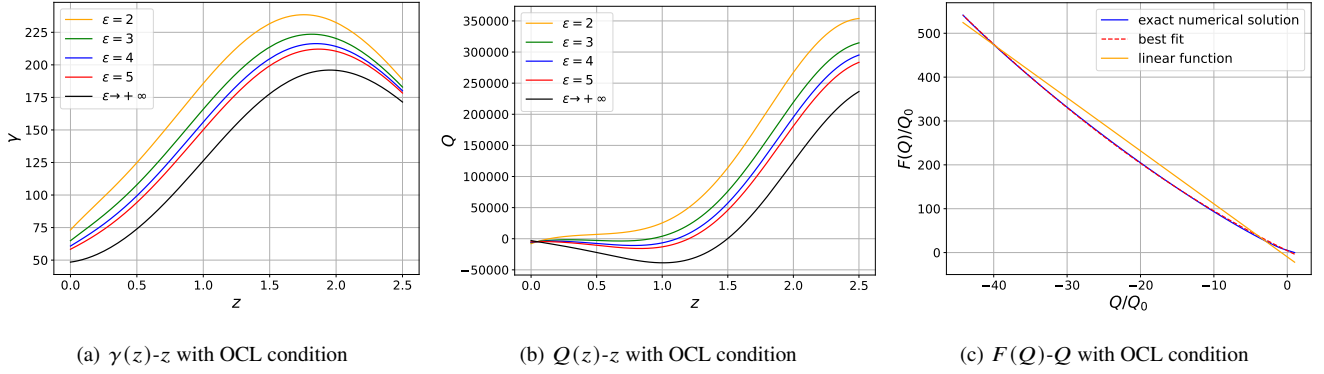


**Figure 2.** The reconstructed  $\gamma(z)$  and  $Q(z)$  for different values of  $\epsilon$  under the assumption of ordinary matter stress-energy tensor conservation law, for the case of Connection II, are shown in Figure 2(a) and Figure 2(b). The reconstructed  $F(Q)$  for  $\epsilon = 2$  are shown in Figure 2(c), where the blue solid curve is the exact numerical solution, the red dashed curve represents the best-fit curve given by  $F(Q) = a_1 + a_2 Q/Q_0 + a_3 Q^2/Q_0^2$ , while the orange line depicts the best-fit linear function  $F(Q) = b_1 + b_2 Q/Q_0$ , namely the STEGR case. The corresponding fitting parameters are  $Q_0 = -8009$ ,  $a_1 = -34614$ ,  $a_2 = 65317$ ,  $a_3 = 724$ ,  $b_1 = 78923$ , and  $b_2 = 96826$ , in  $H_0^2$  units. For the reconstruction, we have used the mean values of  $H(z)$  presented in Figure 1. Without loss of generality for numerical calculation we have set  $B = -5$ .

model with and without an explicit cosmological constant, and for Exp- $f(Q)$  model. Additionally, in the middle panels of Figure 3 we depict the corresponding reconstructed dark-energy equation-of-state parameter  $w_{de}(z)$ . Finally, in the low panels, the reconstructed non-metricity scalar  $Q$  are shown. Similarly, for Connection III, the results are displayed in Figure 4. We mention here that in Gaussian Processes at each specific redshift  $z$  the value of  $H(z)$  exists in the form of a distribution, hence there may be  $H(z)$  values that can cause divergence in the denominator of some terms in the numerical steps, leading to divergences in the reconstructed  $w_{de}(z)$  is some cases.

A first and straightforward observation is that the data-driven reconstructed  $\gamma$  deviate from zero, indicating a deviation from the coincident gauge. Secondly, as we can see the reconstruction results have significantly smaller errors in the case of connection III. Thirdly, we mention that although the Sqrt- $f(Q)$  model in coincident gauge exhibits a degeneracy at the background level for the different model parameter values, and one needs to go at the perturbative level to see distinctive effects, in the case of Connections II and III with a non-zero  $\gamma$ , different  $\alpha$  values lead to different results even at the background level. Interestingly enough, the Sqrt- $f(Q)$  model can fit the data even in the case where  $\Lambda = 0$ , which shows the capabilities in considering non-trivial connections. As for non-metricity scalar  $Q$ , we find that  $Q$  evolves differently under different models, but their absolute values will become smaller and smaller in the future as the universe evolves. Finally, concerning  $w_{de}$ , as we observe it has a tendency to slight phantom values at late times.

We close this section by examining the quality of the fittings. In Table 2 we present the  $\chi^2$  values, alongside the values of the Akaike Information Criterion (AIC), and the Bayesian Information Criterion (BIC). The AIC criterion provides an estimator of the Kullback-Leibler information and it exhibits the property of asymptotic unbiasedness, while and BIC criterion provides an estimator of the Bayesian evidence (Liddle 2007; Anagnostopoulos et al. 2019). Specifically, we have

$$\chi_{model}^2 = \sum_{i=1}^{55} \left[ \frac{(H_{mod,i} - H_{obs,i})^2}{\sigma_{H_i}^2} \right], \quad (38)$$

while

$$AIC = -2 \ln \mathcal{L}_{max} + 2p_{tot} \quad (39)$$

$$BIC = -2 \ln \mathcal{L}_{max} + p_{tot} \ln N_{tot}, \quad (40)$$

where  $H_{mod}$  represents the evolution of the Hubble function corresponding to the specific models with their reconstructed  $\gamma$ . And  $\ln \mathcal{L}_{max}$  represents the maximum likelihood of the model,  $p_{tot}$  represents the total number of free parameters and  $N_{tot} = 55$  is the number of samples. As we can see, our results indicate that the inclusion of  $\gamma$  improves the quality of the fittings to observations, compared to both  $\Lambda$ CDM paradigm, as well as to Sqrt- $f(Q)$  and Exp- $f(Q)$  models under the coincident gauge. This is one of the main results of the present work. Lastly, for completeness we mention that Connection III seems to confront with the data in a slightly better way than Connection II.

## 4 DISCUSSION AND CONCLUSIONS

Recently,  $f(Q)$  gravity has garnered significant attention and has been the subject of extensive research, since its cosmological applications proves to be very interesting. Although the theory has been confronted with observations in order to extract information on the possible forms of the unknown function  $f(Q)$ , almost all the corresponding analyses have been performed under the coincident gauge. Hence, investigating  $f(Q)$  cosmology under different connection choices is a subject both interesting and necessary. In particular, since for general connections that satisfy the torsionless and curvatureless conditions a new dynamical function appears, namely  $\gamma$ , one should study the physical implications and evolutionary characteristics of  $\gamma$ , and try to reconstruct it from the observational data themselves.

In this work we used 55  $H(z)$  observation data to reconstruct the evolution of the dynamical function  $\gamma(z)$  of different connections. In particular, we first applied Gaussian Processes in order to reconstruct  $H(z)$ , and then we expressed  $\gamma(z)$  in terms of  $H(z)$  and the  $f(Q)$  form and parameters. We studied three different connections beyond the coincident gauge, and we were able to reconstruct  $\gamma(z)$  for various cases.

Since in  $f(Q)$  cosmology in general one obtains an effective interaction between geometry and matter, we started our analysis from the case where the ordinary conservation law holds. In this case we extracted a general solution for the derivative of  $f(Q)$ , and utilizing this solution we successfully reconstructed the redshift dependence of  $\gamma(z)$ , revealing a convergence tendency in terms of the model

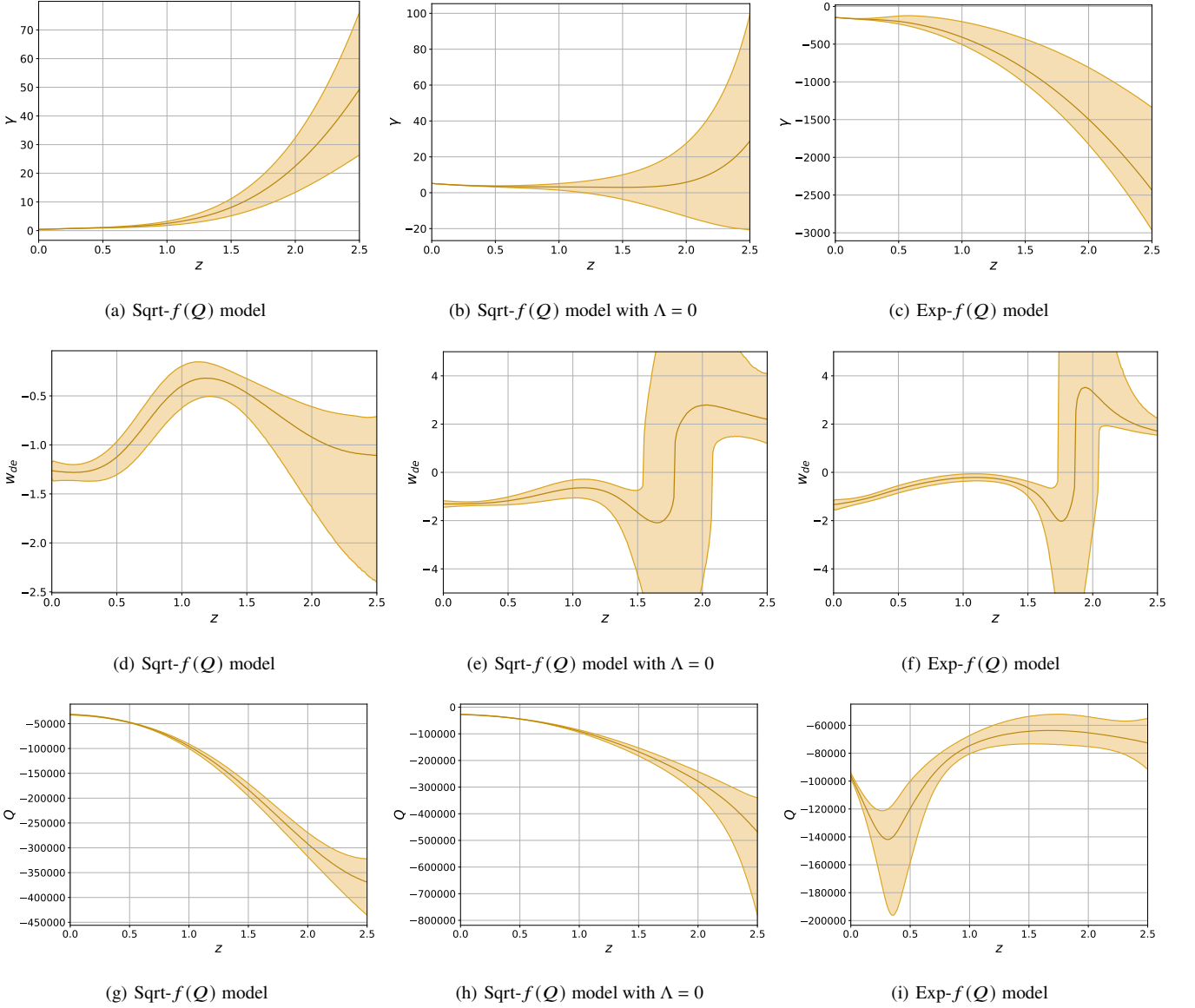


**Figure 3.** The reconstructed  $\gamma(z)$  (upper panels), the corresponding dark-energy equation-of-state parameter  $w_{de}(z)$  (middle panels) and non-metricity scalar  $Q(z)$  (low panels), for the case of Connection II. The left panels correspond to the Sqrt- $f(Q)$  model with  $M = -1500$  (i.e.  $\alpha = -68$ ) and  $\Lambda = 0.7 \times 3H_0^2$  (the  $\Lambda$ CDM value), the middle panels correspond to the Sqrt- $f(Q)$  model with  $M = -5000$  (i.e.  $\alpha = -21$ ) and  $\Lambda = 0$ , while the right panels correspond to the Exp- $f(Q)$  model with  $\beta = 0.2$ , where  $M$  is in  $H_0$  units. The bold curves represent the mean values, while the shaded areas indicate the  $1\sigma$  confidence level.

**Table 2.** The value of  $\chi^2$ , and the information criteria AIC and BIC alongside the corresponding differences  $\Delta IC \equiv IC - IC_{\Lambda\text{CDM}}$ , for different models. Note that for coincident gauge the Sqrt- $f(Q)$  model coincides with  $\Lambda$ CDM scenario at the background level. The Sqrt- $f(Q)$  models with Connection II and III have been taken without an explicit cosmological constant, i.e.  $\Lambda = 0$ .

Model	$\Lambda$ CDM	Coincident gauge		Connection II		Connection III
		Exp- $f(Q)$	Sqrt- $f(Q)$	Exp- $f(Q)$	Sqrt- $f(Q)$	Exp- $f(Q)$
$\chi^2$	139.9	51.6	27.3	27.2	26.2	26.5
AIC	141.9	53.6	31.3	31.2	30.2	30.5
BIC	143.9	55.6	35.3	35.2	34.2	34.5
$\Delta AIC$	0	-88.3	-110.6	-110.7	-111.7	-111.4
$\Delta BIC$	0	-88.3	-108.6	-108.7	-109.7	-109.4

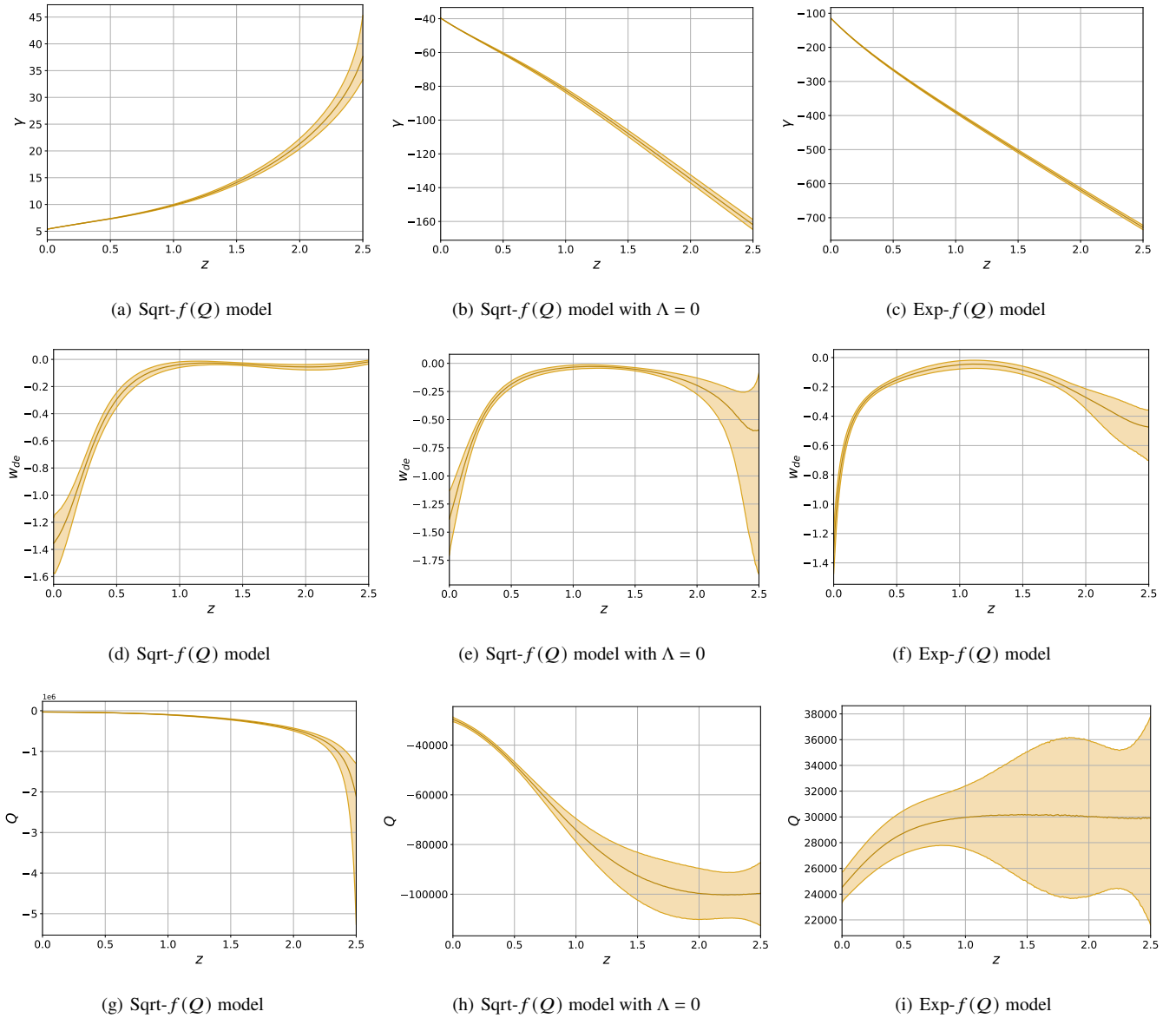


**Figure 4.** The reconstructed  $\gamma(z)$  (upper panels), the corresponding dark-energy equation-of-state parameter  $w_{de}(z)$  (middle panels) and non-metricity scalar  $Q(z)$  (low panels), for the case of Connection III. The left panels correspond to the Sqrt- $f(Q)$  model with  $M = -1500$  (i.e.  $\alpha = -68$ ) and  $\Lambda = 0.7 \times 3H_0^2$  (the  $\Lambda$ CDM value), the middle panels correspond to the Sqrt- $f(Q)$  model with  $M = -5000$  (i.e.  $\alpha = -21$ ) and  $\Lambda = 0$ , while the right panels correspond to the Exp- $f(Q)$  model with  $\beta = 1.2$ , where  $M$  is in  $H_0$  units. The bold curves represent the mean values, while the shaded areas indicate the  $1\sigma$  confidence level.

parameter. Additionally, we reconstructed the corresponding  $f(Q)$  function, which is very well described by a quadratic correction on top of Symmetric Teleparallel Equivalent of General Relativity (STEGR).

Proceeding to the general case, we considered two of the most studied  $f(Q)$  models of the literature, namely the square-root (Sqrt- $f(Q)$ ) one and the exponential (Exp- $f(Q)$ ) one. In both cases we reconstructed  $\gamma(z)$ , and as we showed, the data reveal that  $\gamma(z)$  is not zero. However, the most interesting result is that the quality of the fitting after the inclusion of  $\gamma$  is improved, compared to both  $\Lambda$ CDM paradigm, as well as to Sqrt- $f(Q)$  and Exp- $f(Q)$  models under the coincident gauge. This feature acts as an indication that  $f(Q)$  cosmology should be studied beyond the coincident gauge.

It would be interesting to confront  $f(Q)$  cosmology with non-trivial connections with different observational datasets, such as Su-

pernovae type Ia (SN Ia), Cosmic Microwave Background (CMB), Redshift Space Distortion (RSD) etc, and moreover examine the perturbation evolution. Additionally, it would be necessary to investigate the non-minimal couplings and the direct connection-matter couplings, which are able to make the theories free from pathologies. Such analysis lies beyond the scope of the present work and it is left for a future project.

#### ACKNOWLEDGEMENTS

We are grateful to Bichu Li, Dongdong Zhang, Taotao Qiu, Qingqing Wang, Hongsheng Zhao and Jiaming Shi for helpful discussions and valuable comments. This work is supported in part by National Key R&D Program of China (2021YFC2203100), by CAS



Young Interdisciplinary Innovation Team (JCTD-2022-20), by NSFC (12261131497), by 111 Project (B23042), by Fundamental Research Funds for Central Universities, by CSC Innovation Talent Funds, by USTC Fellowship for International Cooperation, by USTC Research Funds of the Double First-Class Initiative. We acknowledge the use of computing facilities of TIT, as well as the clusters LINDA and JUDY of the particle cosmology group at USTC.

## DATA AVAILABILITY

The data underlying this article will be shared on reasonable request to the corresponding author.

## REFERENCES

- Abdalla E., et al., 2022, *JHEAp*, 34, 49
- Aghanim N., et al., 2020a, *Astron. Astrophys.*, 641, A1
- Aghanim N., et al., 2020b, *Astron. Astrophys.*, 641, A6
- Akrami Y., et al., 2021, Modified Gravity and Cosmology: An Update by the CANTATA Network. Springer (arXiv:2105.12582), doi:10.1007/978-3-030-83715-0
- Alam S., et al., 2017, *Mon. Not. Roy. Astron. Soc.*, 470, 2617
- Albuquerque I. S., Frusciante N., 2022, *Phys. Dark Univ.*, 35, 100980
- Aldrovandi R., Pereira J. G., 2013, Teleparallel Gravity: An Introduction. Springer, doi:10.1007/978-94-007-5143-9
- Anagnostopoulos F. K., Basilakos S., Saridakis E. N., 2019, *Phys. Rev. D*, 100, 083517
- Anagnostopoulos F. K., Basilakos S., Saridakis E. N., 2021, *Phys. Lett. B*, 822, 136634
- Anagnostopoulos F. K., Gakis V., Saridakis E. N., Basilakos S., 2023, *Eur. Phys. J. C*, 83, 58
- Atayde L., Frusciante N., 2021, *Phys. Rev. D*, 104, 064052
- Atayde L., Frusciante N., 2023, *Phys. Rev. D*, 107, 124048
- Bahamonde S., Järv L., 2022, *Eur. Phys. J. C*, 82, 963
- Bahamonde S., Trenkler G., Trombetta L. G., Yamaguchi M., 2023, *Phys. Rev. D*, 107, 104024
- Barros B. J., Barreiro T., Koivisto T., Nunes N. J., 2020, *Phys. Dark Univ.*, 30, 100616
- Beh J.-T., Loo T.-h., De A., 2022, *Chin. J. Phys.*, 77, 1551
- Beltrán Jiménez J., Heisenberg L., Koivisto T. S., 2018a, *JCAP*, 08, 039
- Beltrán Jiménez J., Heisenberg L., Koivisto T., 2018b, *Phys. Rev. D*, 98, 044048
- Beltrán Jiménez J., Heisenberg L., Koivisto T. S., 2019, *Universe*, 5, 173
- Bernardo R. C., Levi Said J., 2021, *JCAP*, 09, 014
- Bhar P., 2023, *Eur. Phys. J. C*, 83, 737
- Bhar P., Malik A., Almas A., 2024, *Chin. J. Phys.*, 88, 839
- Bonilla A., Kumar S., Nunes R. C., Pan S., 2022, *Mon. Not. Roy. Astron. Soc.*, 512, 4231
- Cai Y.-F., Capozziello S., De Laurentis M., Saridakis E. N., 2016, *Rept. Prog. Phys.*, 79, 106901
- Cai Y.-F., Li C., Saridakis E. N., Xue L., 2018, *Phys. Rev. D*, 97, 103513
- Cai Y.-F., Khurshudyan M., Saridakis E. N., 2020, *Astrophys. J.*, 888, 62
- Capozziello S., 2002, *Int. J. Mod. Phys. D*, 11, 483
- Capozziello S., D'Agostino R., 2022, *Phys. Lett. B*, 832, 137229
- Capozziello S., Shokri M., 2022, *Phys. Dark Univ.*, 37, 101113
- Capozziello S., De Falco V., Ferrara C., 2022, *Eur. Phys. J. C*, 82, 865
- Capozziello S., De Falco V., Ferrara C., 2023, *Eur. Phys. J. C*, 83, 915
- Capozziello S., Capriolo M., Nojiri S., 2024, *Phys. Lett. B*, 850, 138510
- D'Agostino R., Nunes R. C., 2022, *Phys. Rev. D*, 106, 124053
- D'Ambrosio F., Heisenberg L., Kuhn S., 2022a, *Class. Quant. Grav.*, 39, 025013
- D'Ambrosio F., Fell S. D. B., Heisenberg L., Kuhn S., 2022b, *Phys. Rev. D*, 105, 024042
- D'Ambrosio F., Heisenberg L., Zentarra S., 2023, *Fortsch. Phys.*, 71, 2300185
- De A., How L. T., 2022, *Phys. Rev. D*, 106, 048501
- De A., Loo T.-H., Saridakis E. N., 2024, *JCAP*, 03, 050
- Delubac T., et al., 2015, *Astron. Astrophys.*, 574, A59
- Di Valentino E., et al., 2021, *Astropart. Phys.*, 131, 102604
- Dimakis N., Paliathanasis A., Christodoulakis T., 2021, *Class. Quant. Grav.*, 38, 225003
- Dimakis N., Paliathanasis A., Roumeliotis M., Christodoulakis T., 2022a, *Phys. Rev. D*, 106, 043509
- Dimakis N., Roumeliotis M., Paliathanasis A., Apostolopoulos P. S., Christodoulakis T., 2022b, *Phys. Rev. D*, 106, 123516
- Dimakis N., Roumeliotis M., Paliathanasis A., Christodoulakis T., 2023, *Eur. Phys. J. C*, 83, 794
- Elizalde E., Khurshudyan M., Myrzakulov K., Bekov S., 2024, *Astrophysics*, 67, 192
- Emtsova E. D., Petrov A. N., Toporensky A. V., 2023, *Eur. Phys. J. C*, 83, 366
- Farooq O., Madiyar F. R., Crandall S., Ratra B., 2017, *Astrophys. J.*, 835, 26
- Ferreira J., Barreiro T., Mimoso J., Nunes N. J., 2022, *Phys. Rev. D*, 105, 123531
- Ferreira J., Barreiro T., Mimoso J. P., Nunes N. J., 2023, *Phys. Rev. D*, 108, 063521
- Frusciante N., 2021, *Phys. Rev. D*, 103, 044021
- Gangopadhyay M. R., Sami M., Sharma M. K., 2023, *Phys. Rev. D*, 108, 103526
- Gomes D. A., Beltrán Jiménez J., Cano A. J., Koivisto T. S., 2024, *Phys. Rev. Lett.*, 132, 141401
- Gonçalves T. B., Atayde L., Frusciante N., 2024, *Phys. Rev. D*, 109, 084003
- Harko T., Koivisto T. S., Lobo F. S. N., Olmo G. J., Rubiera-Garcia D., 2018, *Phys. Rev. D*, 98, 084043
- Heisenberg L., 2024, *Phys. Rept.*, 1066, 1
- Heisenberg L., Hohmann M., Kuhn S., 2023, *Eur. Phys. J. C*, 83, 315
- Heisenberg L., Hohmann M., Kuhn S., 2024, *JCAP*, 03, 063
- Hohmann M., 2020, *Symmetry*, 12, 453
- Hohmann M., 2021, *Phys. Rev. D*, 104, 124077
- Hu Y.-M., Zhao Y., Ren X., Wang B., Saridakis E. N., Cai Y.-F., 2023, *JCAP*, 07, 060
- Huang Y., Zhang J., Ren X., Saridakis E. N., Cai Y.-F., 2022, *Phys. Rev. D*, 106, 064047
- Ikeda S., Saridakis E. N., Stavrinou P. C., Triantafyllopoulos A., 2019, *Phys. Rev. D*, 100, 124035
- Iosifidis D., 2020, *Eur. Phys. J. C*, 80, 1042
- Iosifidis D., 2021, *JCAP*, 04, 072
- Järv L., Pati L., 2024, *Phys. Rev. D*, 109, 064069
- Järv L., Rünkla M., Saal M., Vilson O., 2018, *Phys. Rev. D*, 97, 124025
- Jimenez R., Loeb A., 2002, *Astrophys. J.*, 573, 37
- Kar A., Sadhukhan S., Debnath U., 2022, *Mod. Phys. Lett. A*, 37, 2250183
- Khylllep W., Paliathanasis A., Dutta J., 2021, *Phys. Rev. D*, 103, 103521
- Khylllep W., Dutta J., Saridakis E. N., Yesmakhanova K., 2023, *Phys. Rev. D*, 107, 044022
- Konitopoulos S., Saridakis E. N., Stavrinou P. C., Triantafyllopoulos A., 2021, *Phys. Rev. D*, 104, 064018
- Koussour M., De A., 2023, *Eur. Phys. J. C*, 83, 400
- Krssak M., van den Hoogen R. J., Pereira J. G., Böhrer C. G., Coley A. A., 2019, *Class. Quant. Grav.*, 36, 183001
- Levi Said J., Mifsud J., Sultana J., Adami K. Z., 2021, *JCAP*, 06, 015
- Li M., Zhao D., 2022, *Phys. Lett. B*, 827, 136968
- Li E.-K., Du M., Zhou Z.-H., Zhang H., Xu L., 2021, *Mon. Not. Roy. Astron. Soc.*, 501, 4452
- Liddle A. R., 2007, *Mon. Not. Roy. Astron. Soc.*, 377, L74
- Lovelock D., 1971, *J. Math. Phys.*, 12, 498
- Lu J., Zhao X., Chee G., 2019, *Eur. Phys. J. C*, 79, 530
- Lymperis A., 2022, *JCAP*, 11, 018
- Magana J., Amante M. H., Garcia-Aspeitia M. A., Motta V., 2018, *Mon. Not. Roy. Astron. Soc.*, 476, 1036
- Mandal S., Sahoo P. K., 2021, *Phys. Lett. B*, 823, 136786
- Mandal S., Wang D., Sahoo P. K., 2020, *Phys. Rev. D*, 102, 124029
- Mandal S., Pradhan S., Sahoo P. K., Harko T., 2023, *Eur. Phys. J. C*, 83, 1141
- Maurya S. K., Errehymy A., Jasim M. K., Daoud M., Al-Harbi N., Abdel-Aty A.-H., 2023, *Eur. Phys. J. C*, 83, 317

- Mhamdi D., Bouali A., Dahmani S., Errahmani A., Ouali T., 2024, *Eur. Phys. J. C*, 84, 310
- Mussatayeva A., Myrzakulov N., Koussour M., 2023, *Phys. Dark Univ.*, 42, 101276
- Nájera J. A., Alvarado C. A., Escamilla-Rivera C., 2023, *Mon. Not. Roy. Astron. Soc.*, 524, 5280
- Narawade S. A., Mishra B., 2023, *Annalen Phys.*, 535, 2200626
- Nester J. M., Yo H.-J., 1999, *Chin. J. Phys.*, 37, 113
- Nojiri S., Odintsov S. D., 2005, *Phys. Lett. B*, 631, 1
- Paliathanasis A., 2024, *Phys. Dark Univ.*, 43, 101388
- Paliathanasis A., Dimakis N., Christodoulakis T., 2024, *Phys. Dark Univ.*, 43, 101410
- Papagiannopoulos G., Basilakos S., Paliathanasis A., Savvidou S., Stavrinos P. C., 2017, *Class. Quant. Grav.*, 34, 225008
- Perivolaropoulos L., Skara F., 2022, *New Astron. Rev.*, 95, 101659
- Perlmutter S., et al., 1999, *Astrophys. J.*, 517, 565
- Pradhan A., Dixit A., Zeyauddin M., Krishnannair S., 2024, *Int. J. Geom. Meth. Mod. Phys.*, 21, 2450167
- Quiros I., 2022, *Phys. Rev. D*, 105, 104060
- Ren X., Wong T. H. T., Cai Y.-F., Saridakis E. N., 2021, *Phys. Dark Univ.*, 32, 100812
- Ren X., Yan S.-F., Zhao Y., Cai Y.-F., Saridakis E. N., 2022, *Astrophys. J.*, 932, 2
- Riess A. G., et al., 1998, *Astron. J.*, 116, 1009
- Riess A. G., et al., 2022, *Astrophys. J. Lett.*, 934, L7
- Savvopoulos C., Stavrinos P., 2023, *Phys. Rev. D*, 108, 044048
- Seikel M., Clarkson C., Smith M., 2012, *Journal of Cosmology and Astroparticle Physics*, 2012, 036
- Shabani H., De A., Loo T.-H., 2023, *Eur. Phys. J. C*, 83, 535
- Shabani H., De A., Loo T.-H., Saridakis E. N., 2024, *Eur. Phys. J. C*, 84, 285
- Shi J., 2023, *Eur. Phys. J. C*, 83, 951
- Sokoliuk O., Arora S., Praharaj S., Baransky A., Sahoo P. K., 2023, *Mon. Not. Roy. Astron. Soc.*, 522, 252
- Solanki R., De A., Mandal S., Sahoo P. K., 2022, *Phys. Dark Univ.*, 36, 101053
- Starobinsky A. A., 1980, *Phys. Lett. B*, 91, 99
- Subramaniam G., De A., Loo T.-H., Goh Y. K., 2023, *Fortsch. Phys.*, 71, 2300038
- Wang W., Chen H., Katsuragawa T., 2022, *Phys. Rev. D*, 105, 024060
- Wang Q., Ren X., Wang B., Cai Y.-F., Luo W., Saridakis E. N., 2024, *Astrophys. J.*, 969, 119
- Weinberg S., 1989, *Rev. Mod. Phys.*, 61, 1
- Yan S.-F., Zhang P., Chen J.-W., Zhang X.-Z., Cai Y.-F., Saridakis E. N., 2020, *Phys. Rev. D*, 101, 121301
- Yu H., Ratra B., Wang F.-Y., 2018, *Astrophys. J.*, 856, 3
- Zhang M.-J., Xia J.-Q., 2016, *JCAP*, 12, 005
- Zhao D., 2022, *Eur. Phys. J. C*, 82, 303
- Zhao G.-B., et al., 2017, *Mon. Not. Roy. Astron. Soc.*, 466, 762

This paper has been typeset from a  $\text{\TeX}/\text{\LaTeX}$  file prepared by the author.